Hydrothermal synthesis and photoluminescent characterization of nanocrystalline BaZrO3

L.A. Diaz-Torres*,[a], P.Salas [b], V.M. Castaño[b], J. Oliva [a], E. De la Rosa [a],
a Centro de Investigaciones en Optica A.C., Leon, Gto. 37150 Mexico.
b Centro de Física Aplicada y Tecnología Avanzada, Universidad Nacional Autónoma de México, A. P. 1-1010, Querétaro 76000, Mexico.
* corresponding author: ditlacio@cio.mx.

ABSTRACT

Uniform well faceted sub-microcrystalline $BaZrO_3$ particles have been obtained by a facile hydrothermal reaction. It is found that both morphology and photoluminescence properties depend on reaction time, complexation surfactant, solvent water to ethanol ratio, as well as the coprecipitation agent. Band gap estimations suggest that blue-green emission intensity, under ultraviolet radiation excitation, depends on the degree of crystal lattice disorder. Such disorder degree on turn depends strongly on the coprecipitating agent and post hydrothermal processing annealing time. Morphology depends on coprecipitant agent molarities and reaction times.

Keywords. nanocrystals, Barium zirconate, Hydrothermal method.

1 INTRODUCTION

Since the phenomenon of high temperature protonic conduction in strontium ceramic was discovered by Iwahara et al. in the early 1980s [1], acceptor-doped $A^{2+}B^{4+}O3$ oxides with the perovskite-type structure have been paid much attention because of their potential applications in solid oxide fuel cells, hydrogen sensors, steam electrolysis and catalyst [2]. Recently, more and more investigations were focused on their luminescent properties [3]. Perovskite-type oxides phosphors are very stable and can steadily work in various environments, which is a merit for application. Moreover, Perovskite-type oxides phosphors have been found to be potential candidate in field emission display (FED) and plasma display panel (PDP) devices because they are sufficiently conductive to release electric charges stored on the phosphor particle surfaces [3]. Thus a great deal of perovskite-type oxides phosphors, such as $A^{2+}B^{4+}O3$ (A = Ca, Sr, Ba; B=Ti, Zr, Si, Hf, etc.) [4–6] have been prepared and their luminescent properties were also investigated carefully. Among these, BaZrO3 (BZO) has found interest in a number of applications including as a refractory material, as a structural material in ceramic container crucibles, as components of thermal barrier coatings, as a substrate in the synthesis of superconductors, as pinning centers in superconducting cables, as gate insulator materials, and as high-temperature microwave dielectrics [7-9]. It has been experimentally challenging though to generate uniform, monodisperse particles with reproducible reliability along with simultaneous control over product phase, size, and morphology [10-14]. It has even been difficult to eliminate impurities associated with the products [15]. In this manuscript, we report on the successful preparation of reasonably pure, crystalline, single-phase BaZrO3 submicron regular particles through a simple hydrothermal synthesis method using a alkali salts as precipitants. It is also presented the dependence of morphology and photoluminescence properties on synthesis parameters such as coprecipitant, alkali precipitant concentration, reaction time, and alcohol to water solvent ratio.

2 EXPERIMENTAL CHARACTERIZATIONS

BZO nanoparticles were obtained by hydrothermal process. All chemicals were analytical grade and were used as received. Barium nitrate (Ba(NO3)2), zirconyl chloride octahydrate (ZrOCl2 8H2O), were used as the starting materials for barium zirconate nanoparticles and sodium hydroxide (NaOH) or potassium hydroxide (KOH) were used as the precipitating agents. Cetyl-trimethylammonium-bromide (CTAB) or Pluronic 123 (P123) were used as the surfactants. In a typical procedure, barium nitrate (4.53 g), zirconyl chloride (5.58 g) and CTAB (1.9 g) were dissolved in a solution of ethanol-water at room temperature applying vigorous stirring for 30 min. Under strong stirring, sodium hydroxide was added and stirred again for 1 h at room temperature. The hydrothermal reactions were carried out in a Teflon autoclave (500 ml in total capacity) under autogenous pressure at 100°C for different reaction times, Rt = 2, 6, 12, and 24 h. The precipitate was then washed with distilled water and dried in an oven at 100 °C for 15 h. various water to ethanol solvent ratios, SR, were used with a fixed water volume of 100 ml. Also CTAB was substituted by Pluronic 123, in both surfactant cases the surfactant to BZO molar ratio was 0.3:1; the precipitants (NaOH or KOH) were used with concentration of 1M. Table 1 resumes the different synthesis parameters and the corresponding sample labeling.

The X-ray diffraction patterns of annealed samples were measured in a θ- θ Bruker D-8 Advance diffractometer having the Bragg – Brentano geometry, Cu Kα radiation, a Ni 0.5% Cu-Kβ filter in the secondary beam and a 1-dimensional position sensitive silicon strip detector (Bruker, Lynxeye). Diffraction intensity as a function of the angle 2θ was measured between 20 º and 110º with a 2θ step of 0.01946º and a counting time of 53 s per point. All observed peaks were indexed in correspondence with JCPDS 6-0399 standard for cubic perovskite phase. The morphology of nanocrystals was investigated by Scanning electron Microscopy (SEM) with a JEOL XL30 microscope The optical absorption spectra were obtained with a Perkin-Elmer UV–VIS–NIR Lambda 900 spectrophotometer in diffuse reflectance mode using a 1.5 in integrating sphere (Labsphere Co.). The photoluminescence characterization measurements were performed with a conventional fluorescence setup, the excitation source was a 100W Xe lamp, and the excitation spectrograph, SP300i spectrograph (Acton Research), was setup so the excitation beam had a bandwidth of around 5 nm. The fluorescent emission from the sample was focused onto a SP-500i spectrograph (Acton Research) and detected by a photo multiplier tube R955 (Hamamatsu) connected to a SR830 DSP lock-in amplifier (Stanford Research). All photoluminescence measurements were done at room temperature, and a low band pass filter (cut off at 420 nm) was placed before the emission spectrograph to prevent spurious excitation and its harmonics to reach the detector.

3 RESULTS AND DISCUSSIONS

All synthesized BZO samples, but sample BZ18, have XRD patterns with main characteristic peaks that are in correspondence with JCPDS 6-0399 standard for pure perovskite cubic phase of BZO, see figure 1. The XRD pattern of sample BZ18 presents an amorphous envelope with three main peaks at 24.08°, 30.04°, and 34.34° that correspond to monoclinic zirconia and some other secondary peaks that might correspond to BZO. Samples BZ18, BZ12, and BZ11 represent the BZO crystalline structure evolution with increasing reaction time. From that it is observed that for reaction times of 2h or lower the formed nanoparticles are mainly amorphous precursos of BZO with a small amount of monoclinic zirconia. For reaction times 6h or lager the formed nanoparticles are fully crystallized in the cubic BZO phase, with a small segregation of monoclinic zirconia as is evidenced by the small peak still present at 24.08°. By comparing the BZ11 XRD pattern with the patterns of samples BZ15, BZ16, and BZ22 it is clear that the effects of substituting P123 by CTAB, or KOH by NaOH, or of the change in solvent ratio, are negligible as long as the reaction time is equal or larger than 6h.

SEM micrographs shown that the morphology of the secondary particles depends strongly on reaction time, see figure 2. For reaction times smaller that 2 h the amorphous

Table 1: Synthesis parameters

Sample	Surfactant	Solvent ratio [water : ETOH]	Precipitant	Reaction Time [h]
BZ11	CTAB	4:1	NaOH	24
BZ12	CTAB	4:1	NaOH	6
BZ13	CTAB	4:2	NaOH	24
BZ15	CTAB	4:4	NaOH	24
BZ16	P123	4:1	NaOH	24
BZ17	CTAB	4:1	NaOH	12
BZ18	CTAB	4:1	NaOH	2
BZ20	CTAB	4:4	KOH	2
BZ21	CTAB	4:4	NaOH	2
BZ22	CTAB	4:4	KOH	24
BZ23	P123	4:4	KOH	24

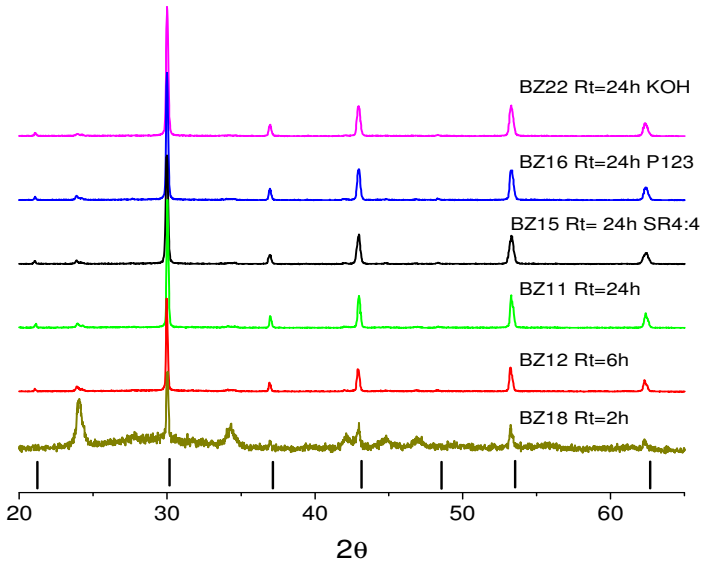

Figure 1. XRD patterns of different BaZrO3 samples as synthesized. See table 1 for the particular synthesis parameters. Bars at the bottom correspond to the JCPDS60399 standard for cibic BaZrO3.

particles are irregular in shape and present a huge size dispersion, see figure 2a. By increasing the reaction time up to 6 h, two main morphologies become present: long needles and spherical like particles, being the needles the dominant morphology. As reaction time increases up to 24 h, sample BZ11, the particles become regular well faceted truncated dodecahedra with an almost monodisperse size distribution around 1.5μm. However there are also many small irregular particles. When the amount of ETOH is increased, with respect to the one used for sample BZ11, to a water to ETOH solvent ratio of 4:4, regular well faceted particles are still observed in sample BZ15 (figure 2d).

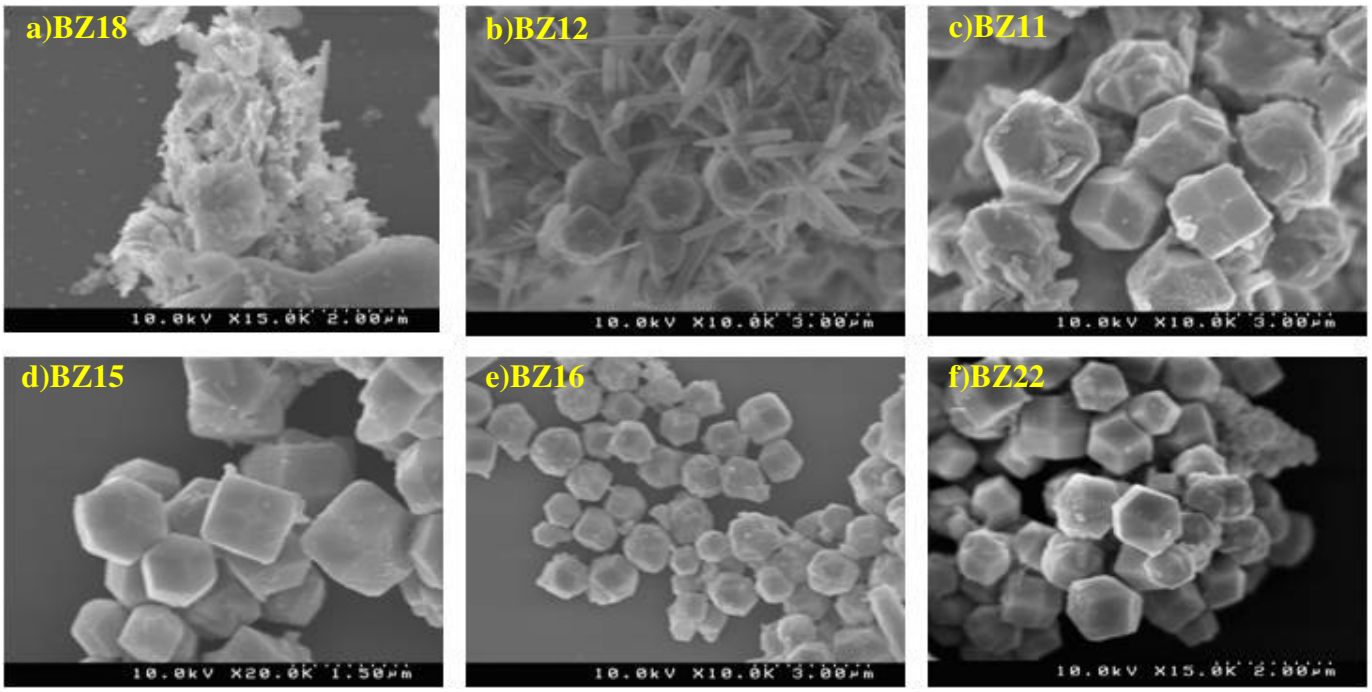

Figure 2. SEM micrographs of BZO samples for different synthesis parameters. See Table 1.

Particles in sample BZ15 are smaller (around 1μm) than the ones in BZ11, also less monodisperse, and a notable fact is that the sample looks cleaner, that is the amount of irregular smaller particles has been greatly reduced with respect to the BZ11 sample. The effect of substituting the surfactant CTAB by P123 results in the formation of smaller and rounder particles, almost sphere like with average sizes of 700 nm, see micrograph of sample BZ16 in figure 2f. On the other side, substitution of the precipitant NaOH by KOH results again in well faceted regular particles of around 600 nm, but in this case there are also a considerable amount of smaller irregular particles, in addition particles in sample BZ22 have huge size dispersion. In summary, the best synthesis conditions in order to obtain clean particles of regular morphology correspond to the ones used for sample BZ15.

Reflectance and wavelength data were converted to Kubelka-Munk [7] (k/s) units and energy in electron volts (eV), respectively. These data were combined in a Tauc plot [8] and the linear region was extrapolated in order to determinate the band gap of the samples in the energy axis, see figure 3. The estimated band gap values were are in the range between 3.907 eV for sample BZ18 and 4.679 eV for sample BZ23. These values are within the range already reported in the literature for pure BZO, from 3.8 to 4.8 eV [9]. The variations on band gap with increasing time suggest that as reaction time increases the crystallinity of the products increases, which is in correspondence with the evolution observed for the main diffraction peak in the XRD patterns in figure 1. The increasing crystallinity might be correlated to a reduction of disorder (increasing band gap) due to the reduction of oxygen vacancies [9]. This also might be correlated with the reduction of the particle sizes as reaction time increases, and the aggregation of smaller irregular particles the larger well faceted particles as observed in figure 2. The estimated band gap values are wide enough to allow transparency for visible and infrared photonic applications.

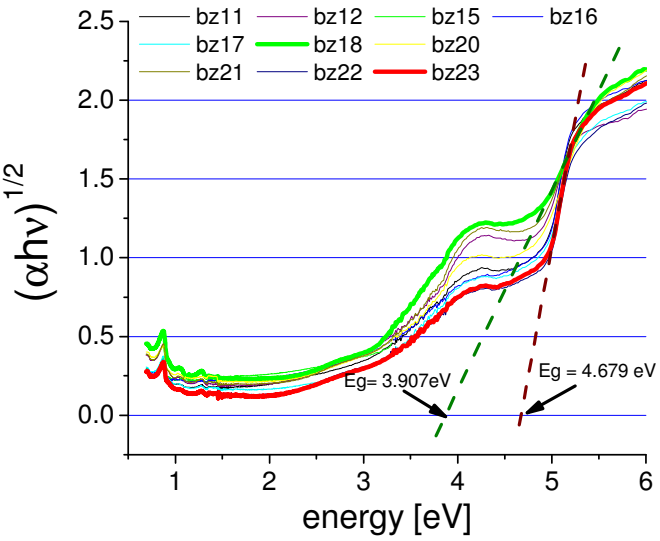

Figure 3. Absorbance spectra of BZO samples in Kubelka-Munk units.

PL spectra have been used widely to examine the efficiency of charge transfer, migration and to understand the behavior of the electron-hole pairs in semiconductors. The BZO samples have a UV to visible broad-band emission (120 nm half width) with to main peaks at about 504 and 552 nm, see figure 4. The excitation spectrum within the region of 220–400 nm has two maximums at about 267 nm and 380 nm, see figure 4a. Their luminescence is mainly caused by the charge transfer transition between the ligand (O^{2-}) and the metal (Zr^{4+}), which belongs to an intrinsic luminescence caused by annihilation of a self-trapped exaction (STE). The excitation peak at 267 nm is caused by the ZrO6–Vo defect center, which yields the emission similar to that of ZrO6 [2, 10]. The observed Stokes blue shift in the emission of BZO respect to previous reported values around 584 nm [10] implies a strong electron-lattice interaction and excitation relaxation in the semiconductor that is related to de increasing degree of order within the crystal lattice. On the other side, the excitation peak at 380 nm might be related to the existence of structural defects within the zirconium octahedral sites, which are an indication of the degree of order-disorder within the BZO crystallites [10]. This might be in agreement with the fact that the PL emission under excitation at 380 nm does not contribute greatly to the 552 nm emission peak.

4 CONCLUSIONS

In summary, we have obtained BZO submicron crystals with well faceted particle morphologies by means of a simple hydrothermal method. The PL properties indicate that in spite of having good level order there are many structural defects that reduce the band gap and promote luminescence centers localized at an excitation energy of 380 nm. It is found that the better synthesis conditions correspond to sample BZ15: water to ethanol solvent ratio 4:4, surfactant CTAB with a molar ratio to BZO of 0.3:1, NaOH at 1M as coprecipitant, and a reaction time of 24 h for the hydrothermal reaction at 100°C under autogenous pressure.

References

[1] H. Iwahara, T. Esaka, H. Uchida, N. Maeda, Solid State Ionics 3/4 (1991) 359.

[2] H. Iwahara, Y. Asakura, K. Katahria, M. Tanaka, Solid State Ionics 168 (2004) 229.

[3] Y. Pan, Q. Su, H. Xu, T. Chen, W. Ge, C. Yang, M. Wu, J. Solid State Chem. 174 (2003) 69–73.

[4] Z. Lu, L. Chen, Y. Tang, Y. Li, J. Alloy Compd. 387 (2005) L1–L4.

[5] N.J. Cockroft, S.H. Lee, J.C. Wright, Phys. Rev. B 44 (1991) 4117.

[6] W.Y. Jia, W.L. Xu, I. Rivera, A. Perez, F. Fernandez, Solid State Commun. 126 (2003) 153.

[7] P. Kubelka and F. Munk, Z. Tech. Phys. (Leipzig) 12, (1931) 593.

[8] J. Tauc, R. Grigorovici and A. Vancu, Phys. Stat. Sol. 15, (1966) 627.

[9] Cavalcante, L. S.; Longo, V. M.; Zampieri, M.; Espinosa, J. W. M.; Pizani, P. S.; Sambrano, J. R.; Varela, J. A.; Longo, E.; Simones, M. L.; Paskocimas, C. A. J. Appl. Phy. 103, (2008) art No. 063527.

[10] M.L. Moreira, J. Andres, J.A. Varela, E. Longo, Cryst. Growth and Design 9, (2009) 833-839.

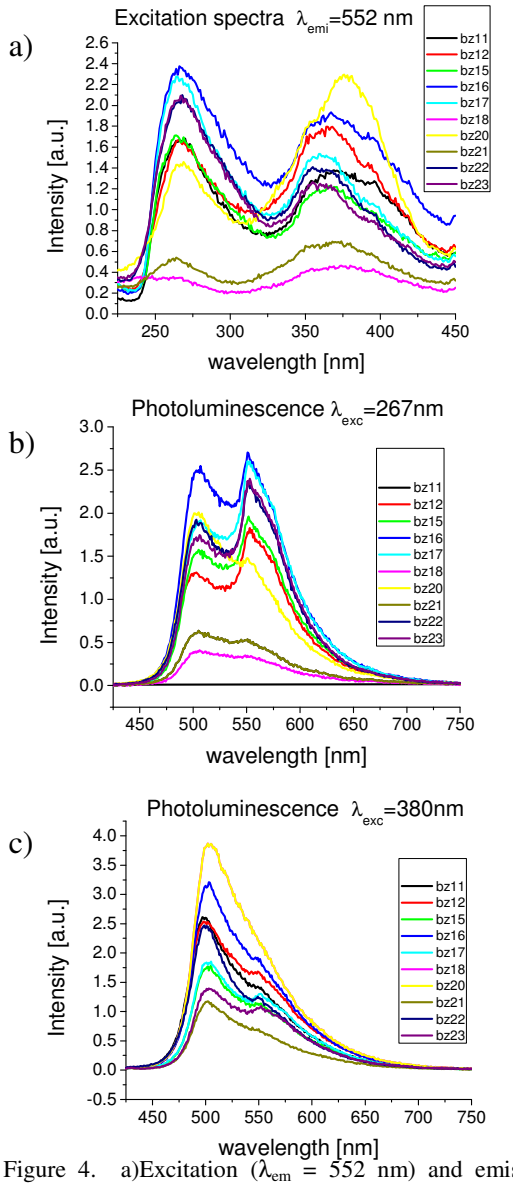

Figure 4. a)Excitation (λ_{em} = 552 nm) and emission spectra at b)λ_{exc} = 267 nm and c)λ_{exc} = 380 nm , of the BZO samples at room temperature.